# Environmental life cycle assessment of novel PV systems for desert conditions

Jose Maria Cruz [a] [iD], Ximena Schmidt Rivera [b,c], Francisca Jalil-Vega [d,*], Raúl O'Ryan [a,e],
Felipe Valencia [f,g], Jorge Rabanal-Arabach [g,h], Eduardo Ayllón Opazo [e],
Paulina Andrea Morris Carmona [e], Patricio Larrain Yañez [e]

[a] Center for Energy Transition (CENTRA), Universidad Adolfo Ibáñez, Santiago, Chile
[b] Department of Chemical Engineering, College of Engineering, Design and Physical Sciences, Brunel University of London, London, UK
[c] Centre for Food Policy, City St George's, University of London, London, UK
[d] UCL Institute for Sustainable Resources, University College London, London, UK
[e] Faculty of Engineering and Sciences, Universidad Adolfo Ibáñez, Santiago, Chile
[f] Facultad de Ciencias de la Ingeniería, Universidad Austral de Chile, General Lagos St 2086, 5111187, Valdivia, Chile
[g] ATAMOSTEC, Uribe 636, 1271616, Antofagasta, Chile
[h] Universidad de Antofagasta, Angamos Avenue 601, 1270300, Antofagasta, Chile

## ARTICLE INFO

## ABSTRACT

Solar photovoltaic (PV) systems are currently seen as an affordable and mainstream renewable energy option to support energy decarbonisation, aligning with commitments of the UN Sustainable Development Goals (SDG 7). This technology prevails in high irradiance places such as deserts, where some of the largest PV systems are installed globally. However, harsh desert conditions reduce PV systems' efficiency and lifespan, among other negative effects. While research on designing PV systems that endure desert conditions is ongoing, little is known about the environmental impacts of these novel PV solutions. This study uses the life cycle assessment (LCA) methodology to assess the environmental impacts of four novel PV system designs (HJT 1–4) for desert conditions and compares them with three systems available in the current market (PERC, PERC+ and TOPCon). The functional unit of the study is 'the production of 1 kWh of electricity AC, considering a PV system connected to a 570kWp grid in the Atacama Desert with a lifespan of 25 years'. The inventories were built using data from tested designs in the desert. 18 environmental impact indicators were included following ReCiPe method, and complemented with energy payback time (EPBT). Results show that the novel design (HJT 3) achieves up to 30% reduction in $GWP_{100}$ per kWh of electricity generated compared to conventional monofacial PERC modules, and a 15% reduction compared to TOPCon modules, primarily due to higher efficiency and reduced materials consumption. The Balance of System (BOS) and installation stage shows the greatest impact on PV systems, contributing 46% on average across all environmental burden, followed by the wafer manufacturing (25% on average) and module manufacturing stages (18% on average). Across all impact categories, including EPBT, PERC is the worst performer, and HJT 3 and HJT 4 are the best performers, followed by TOPCon. This study validates the effort of performing environmental impact assessments on new designs, to ensure both technical performance and the environmental and economic sustainability of renewable energy systems.

## 1. Introduction

The transition to renewable energy is a global priority, driven by the need to mitigate climate change, enhance energy security, and support economic sustainability. Among renewable technologies, solar photovoltaic (PV) systems have emerged as a key solution due to their declining costs and scalability (VDMA, 2021). However, the widespread adoption of PV technologies also presents environmental challenges throughout their lifecycle, including material extraction, manufacturing emissions, and end-of-life disposal concerns (Wu et al., 2024). Addressing these issues requires a region-specific approach that optimises sustainability while maintaining efficiency.

Chile, with its vast solar resources, particularly in the Atacama Desert, presents an ideal setting for solar energy deployment. However, the extreme environmental conditions of this region – high solar irradiance, intense ultraviolet radiation, high variability in daily humidity levels, and substantial temperature fluctuations – accelerate material degradation and increase stress on structures, reducing the operational efficiency and lifespan of standard PV modules (Marzo et al., 2018). Since 2018, the members of the Atacama Module and System Technology Consortium (ATAMOSTEC) have been working on the design of module technologies that withstand these extreme conditions, enhancing durability, and energy yield while minimising environmental impacts (Elias Urrejola et al., 2020).

Using a Life Cycle Assessment (LCA), this study aims to assess the environmental performance in the Atacama Desert of four advanced heterojunction (HJT) PV module designs (HJT 1 to HJT 4), and compare them with commercially dominant technologies. Globally, this evidence will support the strategic development of new PV technologies that better perform in harsh conditions such as of those of desertic regions, which present the most feasible conditions for large scale PV development (Long et al., 2024). Locally, this study provides evidence to inform decision making and practices towards Chile's renewable energy goals and global sustainability standards, ultimately fostering innovation and sustainable practices within the PV industry. The contributions of this study are:

1. The study presents a full set of environmental impacts of these novel technologies under desert conditions, rather than a focus on a few impacts, usually global warming. After 2018 (Gaete-Morales et al., 2018), we have not found studies that use LCA to examine environmental impacts for utility-scale PV systems in Chile, and specifically not under desert conditions.
2. The study tests and assesses improvement opportunities to advance high-radiation PV technologies in preparation of future regulations and requirements of stakeholders.

## 2. Background

### 2.1. Overview of solar cell technologies and trends

A solar photovoltaic (PV) system is composed by a PV panel and Balance of System (BOS) components, which include mounting structures, inverters, transformers, electric conductors, electric controllers, and often these days, batteries. The PV panel is composed by a series of solar cells connected to each other, which transform solar radiation into electricity. The materials these cells are made from depend on the relevant technology, with crystalline silicon (c-Si) accounting for around 95% of global production as for 2021 (International Energy Agency, 2022). Other solar cell materials used generally depend on the cell generation. First generation cells are traditional silicon-based and include mono- (c-Si) and multi-crystalline silicon cells (mc-Si). Second generation cells are thin-layer technologies aiming at lowering materials and production costs – at lower efficiencies – and include amorphous silicon (a-Si), Cadmium telluride (CdTe), or Cadmium sulphide (CdS). Third technology cells aim at improving efficiency and improving manufacturing environmental aspects and include organic and semi-organic cells (OPV), quantum dot-sensitised solar cell, perovskite cells, and dye-sensitised solar cells (DSSC) (Akram Cheema et al., 2024).

Sustained growth trends in manufacturing have led to increased cell conversion efficiencies and lowering material use, which in turn reduces manufacturing costs. Aluminium Back Surface Field (Al-BSF) of mc-Si has been replaced gradually since 2015 by Passivated Emitter and Rear Cell (PERC) technologies (International Energy Agency, 2022). Market share growth of new advanced cell architecture designs, such as heterojunction technology (HJT), interdigitated back contact (IBC), and the current mainstream technology – tunnel oxide passivated contact (TOPCon) – is expected over the next years (VDMA, 2021).

### 2.2. Lifecycle assessment of solar cell technologies

Lifecycle Assessment (LCA) is a method used to assess environmental impacts of products, services, or systems, along its whole lifecycle. A whole lifecycle includes extraction of raw materials, manufacturing, distribution, use phase, and end of life. LCA allows to identify environmental impacts of the various stages of a product or service, under different impact categories. According to ISO 14040/44 guidelines (International Organization for Standardization (ISO), 2006), an LCA is performed in 4 iterative stages, namely, defining the goal and scope of the study, lifecycle inventory (LCI), lifecycle impact assessment (LCIA), and interpretation of results.

PV technologies evolve quickly, and hence LCI databases are frequently outdated. The International Energy Agency (IEA) in its Photovoltaic Power Systems Programme (International Energy Agency, 2024) aims to foster international cooperation to set out main and updated recommendations for LCA of PV systems. The programme recently published a report and dataset (Frischknecht et al., 2020) for performing PV LCAs, together with a set of LCA studies on solar PV. These studies showed that the lifecycle efficiencies of PV technologies evolve rapidly, which underscores the importance of updating and informing changes promptly and frequently.

Previous work on LCA of solar PV systems show the improved environmental performance of new generation technologies, the importance of locational aspects affecting LCAs, and the importance of updating inventories considering fast-paced changes in PV technologies and the broader energy systems. Müller et al. (Müller et al., 2021) compare environmental impacts of single-crystalline silicon glass-back sheet PV systems with newer glass-glass module designs, produced in China and Europe. They find that glass-glass systems show lower environmental impacts than glass-back sheet systems in most impact categories, and lower impacts when produced in the European Union (EU) than in China. They identified module efficiency, energy requirements, silicon consumption and carbon-intensity of the electricity grid during production as pivotal aspects to further reductions in environmental impacts, and stressed the importance of producing updated inventories, especially for electricity mixes. Ullah et al. (Ullah et al., 2025a) present a LCA of monocrystalline and polycrystalline solar PV panels, also in China. They investigate all stages from material collection, through recycling and disposal, showing that monocrystalline panels present higher efficiencies and shorter energy payback (EPBT) times than polycrystalline panels. Ullah et al. (Ullah et al., 2025b) perform an LCA of a 4.6 kWp stand-alone solar PV system in Northern Pakistan, also focusing on location-based EPBT and GHG emissions, considering the socio-economic and regulatory contexts. As this is a stand-alone system, they found that batteries and PV modules are the most GHG-intense components of the system, with PV modules accounting of nearly half of the energy required for manufacturing. Adiansyah et al. (Adiansyah et al., 2025) conducts an LCA on solar PV systems in a mall island in Indonesia, focusing specifically in 2 end-of-life strategies; landfilling and recycling. Maalouf et al. (Maalouf et al., 2023) review LCA studies on thin-film solar cell systems, both commercial and emerging. They analyse 58 thin-film LCA studies and compare them with traditional first-generation silicon-based cells. They found that emerging thin-film technologies outperform commercially available ones in the specified indicators. Overall, their analysis shows that thin-film solar cells require less energy and show a better environmental performance than c-Si solar cell systems, but a EPBT due to their lower efficiencies. Ludin and Mustafa et al. (Ludin et al., 2018) review LCA studies on different PV technologies, considering a cradle-to-grave perspective. Out of silicon cells, thin film cells, dye-sensitised solar cells, perovskite solar cells, and
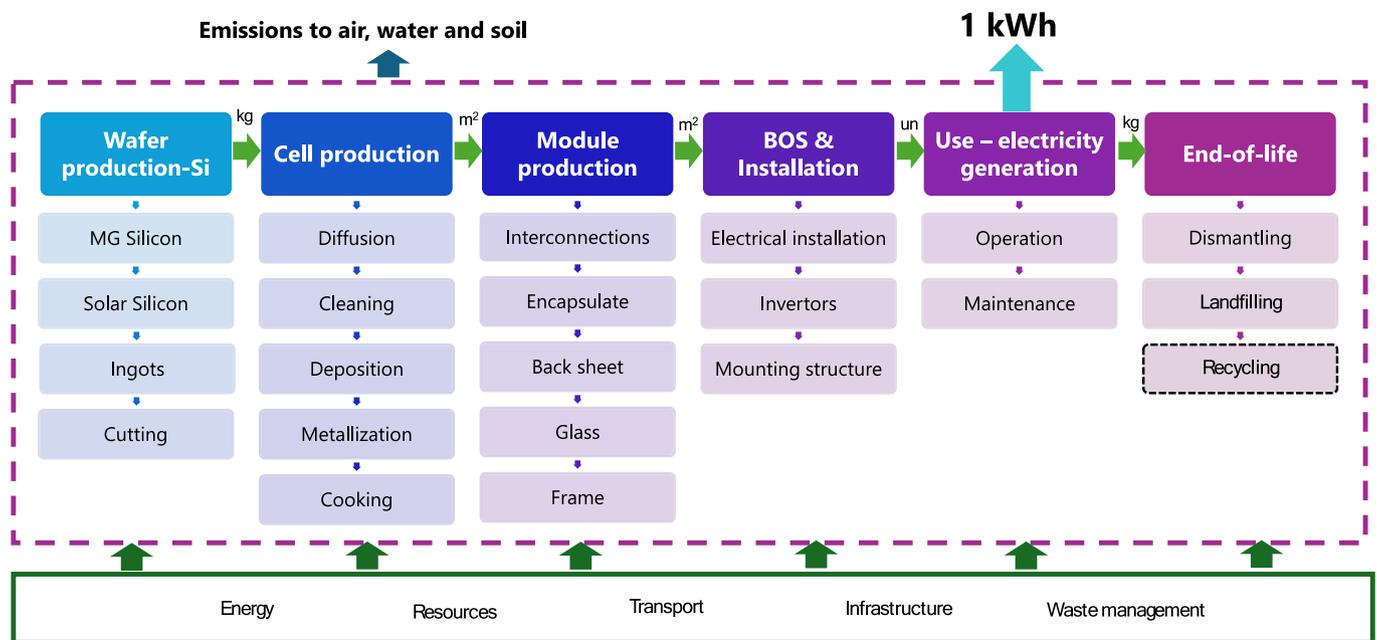
**Emissions to air, water and soil**

**1 kWh**



**Fig. 1.** System boundaries of the PV system including life cycle stage. Each box represents a life cycle stage (darker colour boxes on top row) and their key activities (lighter colour boxes). Arrows show flow of materials, energy and emissions.

quantum dot-sensitised solar cells, mono-crystalline silicon cells were found to perform the worst in terms of energy consumption, energy payback time, and greenhouse gas (GHG) emissions, while dye-sensitised showed the lowest energy consumption and shorter payback time. This study again reinforces the fact that the assessed indicators are sensitive to solar irradiation, module efficiency, and type of technology, as well as to the energy mix of each country where the cells are being produced and used.

While the literature shows many LCA studies of solar PV panels in different locations, very few studies have looked at the environmental impacts of PV systems, novel and or commercially available, using a LCA methodology and assessing a large set of environmental impact categories in desert areas. Those that have explored this have only used commercially available solutions (Ito et al., 2008; Soler et al., 2025). To the best of our knowledge, no prior LCA studies have evaluated frameless HJT modules with smart-wire metallisation in high-irradiance desert regions, nor quantified the environmental benefits of local manufacturing in Chile's low-fossil fuel electricity mix.

This study addresses this gap by assessing the environmental performance in the Atacama Desert of four novel advanced heterojunction (HJT) PV module designs – HJT 1 to HJT 4 of the ATAMOSTEC initiative – using a LCA. These designs incorporate innovative features such as increased bifaciality with respect to commercial modules using the same cell technology, enhanced encapsulation, and frameless configurations, aiming to maximise efficiency and lifespan while minimising their environmental impact. This study also compares these modules to commercially dominant technologies like Passivated Emitter and Rear Cell (PERC), Tunnel Oxide Passivated Contact (TOPCon), and other heterojunction variants. As locational aspects and electricity grid intensity have been shown to be important in lifecycle impacts, we compare the environmental impact of assembling HJT PV modules in Chile, using the local electricity mix, with production in China.

## 3. Methodology

The environmental assessment is carried out using the LCA methodology, following the ISO 14040/44 guidelines (International

Organization for Standardization (ISO), 2006). The next sections detail the four steps of the methodology, starting with the definition of the goal and scope in section 3.1, followed by the life cycle inventory (LCIA) in section 3.2 and then the life cycle impact assessment in section 3.3. The analysis and interpretation of the results are presented in section 4.

### 3.1. Goal and scope

The goal of this study is to examine the environmental performance of four PV systems comprising new PV modules developed by ATAMOSTEC technology – HJT 1–4, especially designed to perform in desert conditions – and to identify and test improvement opportunities to enhance their environmental sustainability. A further goal is to compare these new designs with three commercially available PV technologies, namely, PERC, PERC+, and TOPCon. A description of the PV systems is depicted in section 3.1.1.

The functional unit is detailed as the production of 1 kWh of AC electricity, considering a PV system connected to a 570kWp grid in the Atacama Desert with a lifespan of 25 years. The assessment accounts for the PV-systems' whole life cycle, considering the extraction of raw materials, the manufacturing of the PV cells, and all the equipment required to operate the PV system. The use phase and end-of-life (EoL) stages of all components – including waste management and recycling practices – are also included, as well as the transport required for all resources and components of the system. Thus, the scope of the study is from cradle to grave. Fig. 1 shows the system's boundaries, including key components and life cycle stages. The life cycle stages have been defined in a way that enables the assessment of each critical component to inform manufacturers and decisionmakers on improvement opportunities. Section 3.2 offers a detailed description of each stage and their inventory analysis.

#### 3.1.1. Description of the PV modules

The ATAMOSTEC Heterojunction Technology (HJT) (Atamostec, 2023) has been developed in Chile through public-private investment, involving local and international efforts to adapt the technology to harsh desert conditions. The technology focuses on designing modules with

**Table 1**
Characteristics and key parameters of the studied PV systems.

| Life cycle stage | Parameter | Unit | PERC [a, c, f] | PERC+ [a,c] | TOPCon [a,d] | HJT 1 [a,c,e,f] | HJT 2 [a,b,e,f] | HJT 3 [a,b,e,f] | HJT 4 [a,b,e,f] |
|---|---|---|---|---|---|---|---|---|---|
| | Reference Model | | KOSOL ENERGIE PVT. LTD. KE345M | Longi LR4-72HBD-440 M | JOLYWOOD JW-HD144N | Adapted to local conditions | Adapted to local conditions | Adapted to local conditions | Adapted to local conditions |
| Wafer | Manufacturing year | Year | 2018 | 2020 | 2022 | 2018 | 2019 | 2019 | 2019 |
| Cell | Cell architecture | – | PERC | PERC+ | TOPCon | HJT | HJT | HJT | HJT |
| | Power | kW$_P$ | 570 | 570 | 570 | 570 | 570 | 570 | 570 |
| | Exit power | W$_P$ | 344 | 440 | 550 | 355 | 383 | 388 | 383 |
| | Bifacial factor | % | N/A | 70 | 75 | 88.2 | 90 | 91 | 91 |
| | Efficiency | % | 17.46 | 20.24 | 21.23 | 17.94 | 18.85 | 19.10 | 18.85 |
| Module | Area | m$^2$ | 1.97 | 2.17 | 2.59 | 1.98 | 2.03 | 2.03 | 2.03 |
| | Weight | Kg | 32 | 27.5 | 32.5 | 32 | 35 | 35 | 35 |
| | | kg/m$^2$ | 16.23 | 12.65 | 12.54 | 16.17 | 17.25 | 17.25 | 17.25 |
| | Frame materials | – | Frameless | Aluminium | Aluminium | Frameless | Frameless | Frameless | Frameless |
| | Frame weight | kg/m | 2.13 | 2.13 | 2.13 | 0 | 0 | 0 | 0 |
| | Cover materials | front /back | Glass / back sheet | Glass / Glass | Glass / Glass | Glass / Glass | Glass / Glass | Glass / Glass | Glass / Glass |
| | Thickness of cover | Mm | 3 | 2 | 2 | 3 | 3 | 3 | 3 |
| | Thickness | Mm | N/A | 2 | 2 | 3 | 3 | 3 | 3 |
| | Encapsulant type | – | POE | POE/EVA | POE | TPO | POE | POE | POE |
| | Encapsulant weight | g/m$^2$ module | 849 | 849 | 849 | 849 | 849 | 849 | 849 |
| | Number of cells | – | 72 | 144 | 144 | 72 | 144 | 144 | 72 |
| | Cell cut type | – | full | half | half | full | Half | half | full |
| | Cell size | Mm | 156.75 × 156.75 | 166 × 83 | 182 × 91 | 156.75 × 156.75 | 156.75 × 78.375 | 156.75 × 78.375 | 156.75 × 78.375 |
| | M series | | M2 | M6 | M10 | M2 | M2 | M2 | M2 |
| | Metallisation pattern | | 5BBs | MBB (9BB) | MBB (11BB) | 4BBs | 6BBs | MBB (18BB) | MBB (18BB) |
| | Wafer doping (substrate) | | p | n | n | n | n | n | n |
| | Lifespan | Year | 25 | | | | | | |

**POE:** Polyolefin elastomer; **EVA:** Ethylene Vinyl Acetate; **TPO:** Thermoplastic Polyolefin; **BB:** busbars: **MBB:** Multi – busbars.
Note: Extra details of the inventories upon request.
[a] IEA PVPS 2020 LCI (Frischknecht et al., 2020), UVEK LCI DQRv2:2018 (KBOB, 2024; Ecoinvent, 2023).
[b] ITRPV 2020 (VDMA, 2020).
[c] ITRPV 2019 (VDMA, 2019).
[d] ITRPV 2022 (VDMA, 2021).
[e] BOM ATAMO I y II.
[f] LCA of Heterojunction Solar Cells (Alexis, 2022).

enhanced performance adapted to cope with extreme environmental conditions, specifically high irradiation and overall harsh desert settings (e.g., large daily temperature oscillations). It has also included a circular economy approach enabling second life use and remanufacturing of the modules (Elias Urrejola et al., 2020).

The module developed within the ATAMOSTEC consortium (ATAMO module) incorporates a n-type HJT cell (Elias Urrejola et al., 2020) that combines a crystalline silicon wafer with thin layers of amorphous silicon on both sides. This architecture enhances efficiency by improving light absorption and reducing electron recombination losses, while also providing excellent performance under high temperatures and strong resistance to UV radiation and environmental stress. The module uses an advanced encapsulation technique to enhance its durability and efficiency. The ATAMO module has been tested for over a year in the Atacama Desert (Lelièvre et al., 2022). Some of the key features of the ATAMO HJT modules include:

- *Resistance to environmental stress:* The modules are tested under ultra-accelerated aging protocols that simulate the harsh conditions of the Atacama Desert, including high UV radiation, thermal cycling, and salt mist exposure. These tests ensure that the modules can withstand severe environmental stress while maintaining stable performance.
- *Improved stability and performance:* The HJT modules exhibit a slight increase in all performance parameters during testing, indicating a

low dispersion in performance and a high level of reliability. The use of specific encapsulant materials has shown to effectively preserve the cells' performance by reducing the impact of UV radiation and other environmental factors.

For this study, four versions of the ATAMO modules were selected: HJT 1, HJT 2, HJT 3, and HJT 4. These versions were developed based on the performance results of the HJT 1 module, which was exposed to the extreme environmental conditions of the Atacama Desert characterised by high UV irradiance and significant intra-day temperature and humidity fluctuations. Due to the high sensitivity of the HJT 1 cells to UV radiation observed in field tests, the TPO encapsulant used in HJT 1 was replaced in all subsequent versions (HJT 2–4) with POE encapsulants with UV blockers. In addition, modifications were made to both the cell-cut types and the metallisation patterns across the new versions. Specifically, the HJT 2 version features six busbars – an increase from the four used in HJT 1 – and adopts a half-cell as the cell-cut type. HJT 3 employs smart wire contacting technology as the metallisation pattern, and also uses half-cells. HJT 4 similarly incorporates smart wire technology as the metallisation pattern, but utilises full-cell design. In both HJT 3 and HJT 4, the smart wire contacting technology consists of copper wires supported by a polymer foil. These wires are coated with a thin layer of low melting point alloy, which melts during the lamination process to form soldered contacts with the cell metallisation (Faes et al.,

2014).

ATAMO modules are compared with current market competitors - Passivated Emitter and Rear Cell (PERC, PERC+) and Tunnel oxide passivated contact (TOPCon). These technologies were chosen based on current and projected market shares (ACERA A.G., 2023; Coordinador Eléctrico Nacional, 2023). PERC and PERC+ technologies represented ~75% of the global market in 2023.TOPCon represented 10% of the market in the same year, and present an expected growth to 60% by 2033 (ACERA A.G., 2023). Additionally, PERC+ was studied because it is the most popular technology installed in Chile (ACERA A.G., 2023; Coordinador Eléctrico Nacional, 2023). The information of these modules was obtained from literature, manuals and patterns. Table 1 shows the characteristic and key parameters of the seven PV systems assessed in this study.

### 3.2. Life cycle inventory (LCI)

The inventory was built using academic literature, manuals and industry reports. Data to model the ATAMO HJT systems' life cycle was collected directly from the manufacturer. The Ecoinvent 3.9.1 dataset for 'Photovoltaic panel, single-Si, at plant' (representing Al-BSF technology) was used as the baseline proxy (Ecoinvent, 2023), together with the model developed by IEA (PVPS 2020 LCI (Frischknecht et al.,

**Table 2**
Summary of key adaptations of Ecoinvent models.

| Life cycle stage | Summary of key adaptations of Ecoinvent models |
| --- | --- |
| **Wafer manufacturing** | Changes in production line to reflect manufacturing in China using Siemens's process, and the corresponding national utilities. Linear scale of background models to match the specific wafer thickness of each technology (see section 3.2.1, Table 1, Table 3). |
| **Cell manufacturing** | Changes in metallisation and energy inputs for each model. For the HJT 3 (Smart-Wire), the aluminium back-paste was eliminated, and silver paste consumption was adjusted to reflect the 18BB wire technology, setting inputs to 1.23 g/m² (front) and 2.86 g/m² (back). Electricity consumption for the cell process was updated to 12.00 kWh/m² for the HJT variants. Detailed explanations in section 3.2.2 and Table 4. |
| **Module manufacturing** | Changes to represent Atacama Desert (Chile) conditions and supply chain aspects. Module assembly was restructured to use a glass-glass configuration for the HJT designs, and its configuration was integrated by modifying the 'Solar glass' input (increased to 15.6 kg for HJT 3). The encapsulant inputs were modified to Polyolefin Elastomer (POE) used in HJT modules. See section 3.2.3 and Table 1 for detailed description and comprehensive summary. |
| **Balance of systems (BOS) and installation** | A 500 kW inverter was included, considering a life span of 30 years, and a replacement of 10% in weight every 10 years. For all other components, construction and transport inputs were scaled according to the specific area (m²) and local logistic distances (km). See details in section 3.2.4. |
| **Use stage** | The electricity generation was modelled year-by-year using SAM software, considering the specific degradation rates and bifacial gains. Details of the parameters used and results in Table 5, and explanations in section3.2.5. |
| **End-of-life** | Waste management option of the cells at the end of their life span, considered as 25 years. In Chile, the current end of life practices for PV systems is still landfill, which was used as default for this study. Ecoinvent 3.9.1 models were modified by adding landfill for specific materials e.g., glass, aluminium, etc. Recycling options were also explored as part of the scenario analysis (in section 4.2). See details in section 3.2.6. |

2020)), and UVEK LCI DQRv2:2018 (KBOB, 2024). To ensure this generic dataset accurately reflects the specific novel technology features of HJT and market-competitor modules, a systematic parametric adaptation was applied to the key unit processes, each of which are explained in the following sections. The models were adapted to reflect local conditions and supply chains. SAM Software (NREL, 2024) was used to determine key parameters representative of local conditions. The following sections describe each life cycle stage and their components, including data used and assumptions made. A summary of the key adaptations made to the baseline models are presented in Table 2.

#### 3.2.1. Wafer manufacturing

This stage accounts for all the processes necessary to produce the wafer, including the extraction and production of the raw materials, the extraction and production of silicon, and its further transformation to solar grade silicon and then single crystalline silicon. Transportation of raw materials is also included in this process. High purity silicon, also known as metallurgic grade silicon, is the key components of the cell, which is further purified to get to solar grade, and crystalised to generate monocrystalline silicon through the Czochralski process (Cz-Si). Solar grade silicon is thinly sliced to produce silicon wafers.

The input of 'CZ single crystalline silicon', from Ecoinvent 3.9.1, was linearly scaled to match the specific wafer thickness of each technology. Based on the inventory data, the baseline consumption of the proxy (0.595 kg Si/m² for a standard 175 μm wafer) was adjusted down to 0.560 kg Si/m² for the HJT 3 design (160 μm), reducing the silicon intensity of the novel modules. It is important to highlight that although the ATAMO HJT technology has been designed, produced and tested in Chile, it is expected to be manufactured in China. The wafer production system was sourced from Ecoinvent 3.9.1, specifically the 'photovoltaic panel, single-Si, at plant/m2/CN/I U', modified to represent the production line in China using Siemens's process, and the corresponding national utilities, e.g., electricity mix, water, heat, etc. Table 3 shows energy consumption used to model each technology, adapted using the thickness of the wafer.

#### 3.2.2. Cell manufacturing

After wafers are produced, they are transformed into solar cells through a variety of processes and methods depending on the technology of the module. In general, this process accounts for texturing and cleaning (alkaline process), p-n union diffusion or doping, and chemical and physical deposition in vapour phase. After this, the metallisation process enables the electrical contact points of the module. Finally, the modules are cooked and cured to enable the ensemble with the wafer.

Significant modifications were made to the metallisation and energy inputs to reflect the HJT architecture compared to the Al-BSF base. For

**Table 3**
Electricity consumption per technology (Frischknecht et al., 2020; KBOB, 2024; Ecoinvent, 2023).

| Parameter | Unit | PERC | PERC+ | TOPCon | HJT 1 | HJT 2–4 |
| --- | --- | --- | --- | --- | --- | --- |
| Electricity used for MG-Si manufacturing | kWh/kg MG-Si | 11 | 11 | 11 | 11 | 11 |
| Electricity used for SoG-Si manufacturing | kWh/kg SoG-Si | 49 | 49 | 49 | 49 | 49 |
| Electricity used for CZ-Si block manufacturing | kWh/kg CZ-Si | 35 | 30 | 27 | 35 | 32 |
| Electricity used for wafer manufacturing | kWh/m² wafer | 4.76 | 4.76 | 4.76 | 4.76 | 4.76 |
| Wafer thickness | um | 175 | 170 | 155 | 165 | 160 |
| Wafer substrate | | p | n | n | n | N |

Note: specific inventories upon request.

**Table 4**

Cell manufacturing stages per cell architecture (Alexis, 2022; Molto et al., 2023; Song and Deng, 2022; Söderströma et al., 2013).

| Process | PERC | PERC+ | TOPCon | HJT |
|---|---|---|---|---|
| Cleaning, damage removal from sawing and texturing | ✔ | ✔ | ✔ | ✔ |
| Diffusion of the p-n junction | ✔ | ✔ | ✔ | x |
| | (POCl$_3$) | (BBr$_3$) | (BBr$_3$) | |
| Cleaning by immersion in hydrofluoric acid (HF) | ✔ | ✔ | ✔ | x |
| Chemical and physical deposition in vapour phase | ✔ | ✔ | ✔ | ✔ |
| | (SiNx & AlOx) | (SiNx & AlOx) | (SiNx & AlOx, poli-Si/SiOx) | a-Si:H & TCO |
| Metallisation | ✔ | ✔ | ✔ | ✔ |
| | (Ag front & Al back) | (Ag front & Al back) | (Ag both) | (Ag both) |
| Co-cooking and curing | 850 °C | 850 °C | 850 °C | 230 °C |

Note: specific inventories upon request.

instance, for the HJT 3 (Smart-Wire), the aluminium back-paste was eliminated (set to 0 kg, compared to 0.055 kg in the base model). Instead, silver paste consumption was adjusted to reflect the 18BB wire technology. Inputs were set to 1.23 g/m$^2$ (front) and 2.86 g/m$^2$ (back). This represents a significant reduction compared to the HJT 1 baseline, which required ~9.0 g/m$^2$ of silver paste. For process energy, electricity consumption for the cell process was updated based on primary data, reducing from 17.75 kWh/m$^2$ in the base model to 12.00 kWh/m$^2$ for the HJT variants, reflecting the lower thermal loads of heterojunction processing (e.g., lower curing temperatures).

Table 4 details the processes involved for each cell architecture. Ecoinvent 3.9.1's module 'photovoltaic panel, single-Si, at plant/m2/ CN/I U' was used as background data, modified to represent the characteristics of each system as per cell architecture (see Table 4).

### 3.2.3. Module manufacturing

The module manufacturing process starts with cells being set in strings and then inserted in a glass based bifacial module where they are connected, laminated, and encapsulated, using polymers like Ethylene Vinyl Acetate (EVA) or Polyolefin Elastomer (POE). Glass is set in the front or backs, depending on the model. Electrical connexions are attached, and depending on the model, aluminium frames are jointed.

The Ecoinvent 3.9.1's module '570 kWp open ground installation, multi-Si, on open ground/p/ES/I U' for Spanish conditions was modified to represent of those of the Atacama Desert (Chile), together with supply chain aspects such as distance from manufacturers, electricity mix, etc.

Significant changes were made to the Ecoinvent database in order to represent the technologies in this study. For instance, the inventory of the module assembly was restructured to switch from a glass-back sheet to a glass-glass configuration for the HJT designs. For the frameless design, the input for 'Aluminium alloy, AlMg3', which accounts for 2.13 kg/module in the base and PERC scenarios, was set to zero for all ATAMO HJT designs. The glass-glass configuration was integrated by modifying the 'Solar glass' input, which was increased from ~8.8 kg (base) to 15.6 kg for HJT 3, accounting for the double-glass structure essential for bifaciality and durability.

To account for the desert-adapted encapsulant, the encapsulant inputs were modified to model the specific Polyolefin Elastomer (POE) used in HJT modules. Unlike standard EVA, this material is specially designed with a high UV cut-off to withstand the harsh UV irradiation of the Atacama Desert. Table 1 summarises key parameters used for modelling the modules.

### 3.2.4. Balance of system (BOS) and auxiliary equipment

This stage includes the production and installation of the inverter to convert DC to AC current. A 500 kW inverter was included, considering a life span of 30 years, and a replacement of 10% in weight every 10 years, as suggested by (Frischknecht et al., 2020). The modules require a mounted structure made of aluminium, steel and concrete. An essential part of the system are cables and electric conductors as they enable the interconnection of the system with the PV modules.

Ecoinvent 3.9.1 was used for background data, which include the extraction and production of the raw materials and the transportation of

them between stages, as well as all the energy and materials required for the manufacturing of each component and their end of life. The module for a '570 kWp open ground installation, single-Si' was used and modified to represent each system. The 'Inverter, 500kW, at plant' module was used for the inverter, and the 'electric installation, 570 kWp photovoltaic plant, at plant' and 'open ground construction, on ground' modules were used for the electric installation and structure, respectively.

To reflect the local context, the 'Open ground construction' and transport inputs were scaled according to the specific area (m$^2$) and local logistic distances (km) using data of a project located in the Atacama Desert.

### 3.2.5. Use stage

This stage includes the energy generated across the life span of the system, which was determined using the System Advisor Model (SAM) (NREL, 2024) applying the simple efficiency module model, following guidelines from (Gilman, 2015). The electricity generation was modelled year-by-year using SAM software, considering the specific degradation rates and bifacial gains (e.g., HJT 3 generation starting at ~1.42 GWh/year for the total system). Table 5 summarises the key parameters used for determining the total energy generated.

### 3.2.6. End-of-life stage

This stage accounts for the waste management option of the cells at the end of their life span, considered as 25 years. In Chile, the current end of life practices for PV systems is still landfill, which was used as default for this study. For this purpose, the module 'treatment, c-Si PV module/kg/RER U' from Ecoinvent 3.9.1 was used, together with those of landfill for specific materials such as 'Disposal, glass, 0% water, to inert material landfill/CH U', 'Disposal, aluminium, 0% water, to sanitary landfill/CH U'. Recycling options were further studied as part of the scenario analysis in Section 4.2.

### 3.2.7. Allocation

System expansion has been used to account for the avoidance burden of recycling materials (section 4.2 - scenario analysis). Ecoinvent 3.9.1 database was used for these purposes, using the following modules:

- Glass: Flat glass, uncoated, at plant/RER U
- Aluminium: aluminium, primary, at plant/kg/RER U
- Copper: Copper, primary, at refinery/RER U
- Steel: Steel, low-alloyed, at plant/RER U

### 3.3. Life cycle impact assessment (LCIA)

The life cycle impact assessment is carried out using OpenLCA software, v2.02 (OpenLCA, 2025), applying an attributional approach. ReCiPe 2016 (Huijbregts et al., 2017) was selected as impact assessment method, using the hierarchical approach (H), and including 18 environmental impacts, grouped in four categories: resource scarcity, air pollution, water and soil pollution, and toxicities. Climate change (GWP$_{100}$) is the only impact that has been left stand-alone due to its

**Table 5**
Key parameters to calculate generated electricity.

| Parameter | Unit | PERC[a,b] | PERC+[a,b] | TOPCon[a,b] | HJT 1[a,b,c] | HJT 2[a,b,c] | HJT 3[a,b,c] | HJT 4[a,b,c] |
|---|---|---|---|---|---|---|---|---|
| Global irradiation 24° PSDA | kWh/m$^2$/year | 2719.25 | | | | | | |
| Albedo | % | 30 | | | | | | |
| Performance coefficient (PR) | | 0.8 | 0.85 | 0.86 | 0.87 | 0.88 | 0.88 | 0.88 |
| Temperature coefficient Pmax (Pmp) | %/°C | −0.38 | −0.331 | −0.32 | −0.26 | −0.26 | −0.26 | −0.26 |
| Degradation in Y1 STC | % | 2% | 2% | 1% | 1% | 1% | 1% | 1% |
| Annual Degradation STC | % | 0.70 | 0.50 | 0.40 | 0.40 | 0.40 | 0.40 | 0.40 |
| Plant factor | | 0.274 | 0.262 | 0.28 | 0.284 | 0.284 | 0.284 | 0.285 |
| Total energy produced | GWh | 31.24 | 29.85 | 33.24 | 34.23 | 34.28 | 34.28 | 34.3 |

Note: specific inventories upon request.
[a] IEA PVPS 2020 LCI (Ullah et al., 2025a), UVEK LCI DQRv2:2018 (KBOB, 2024).
[b] Albedo Desierto de Atacama (Cordero et al., 2021), Solar Advisor Model (SAM) NREL (NREL, 2024).
[c] BOM ATAMO I y II.

current importance. The indicators accounted for in each group are the following:

- *Resource scarcity* includes mineral resource scarcity (SOP), fossil resource scarcity (FFP), land occupation (LOP) and water consumption (WCP).
- *Air pollution* accounts for stratospheric ozone depletion (ODP), particulate matter formation (PMFP), ecosystem damage ozone formation (EOFP) and Human damage ozone formation (HOFP).
- *Water and soil pollution* represents terrestrial acidification (TAP) and freshwater (FEP) and marine (MEP) eutrophication.
- *Toxicities* incudes human carcinogenic (HTPc) and noncarcinogenic toxicity (HTPnc), terrestrial ecotoxicity (TET), freshwater ecotoxicity (FETP), marine ecotoxicity (METP), and ionising radiation (IRP).

To complement the 18 environmental impacts and to account for the time for energy recovery, this study includes a 19th indicator – the energy payback time (EPBT), measuring the time required for a PV system to generate the energy consumed during its life cycle. A shorter EPBT indicates greater efficiency and sustainability.

## 4. Results and discussion

The environmental impact assessment of all technologies and their comparison are presented in section 4.1, discussed by group. Then a scenario analysis will be discussed on section 4.2, followed by a sensitivity analysis in section 4.3. Finally, the validation of the results is analysed in section 4.4.

### 4.1. Environmental impacts

The environmental impacts of the evaluated PV systems are comprehensively summarised in Table 6 and Table 7. Among all the technologies evaluated, the PERC system presents the highest environmental impacts in all impact categories. In contrast, the HJT 3 technology emerges as the most sustainable option, exhibiting the lowest

**Table 6**
Environmental Impacts of PV systems for desert conditions - Climate change, Resource Scarcity and Air Pollution.

| Group | Impact Category | Acronym [Unit] | PERC | PERC+ | TOPCon | HJT 1 | HJT 2 | HJT 3 | HJT 4 |
|---|---|---|---|---|---|---|---|---|---|
| | Climate Change | GWP$_{100}$ [g CO$_2$ eq] | 25.6 | 19.4 | 17.8 | 18.8 | 17.9 | 17.6 | 17.8 |
| **Resource Scarcity** | Mineral resource scarcity | SOP x 10 [mg Cu eq] | 17.1 | 14.2 | 13.6 | 16.9 | 16.3 | 12.7 | 12.8 |
| | Fossil resource scarcity | FFP [g oil eq] | 5.7 | 4.3 | 4 | 4.3 | 4.1 | 4.1 | 4.1 |
| | Land use | LOP x 10 [cm$^2$ y eq] | 11.8 | 9.3 | 8.7 | 10 | 9.5 | 9.4 | 9.5 |
| | Water consumption | WCP x 10 [L] | 8.3 | 6.4 | 5.9 | 6.1 | 5.8 | 5.7 | 5.8 |
| **Air Pollution** | Ozone depletion | ODP [μg CFC$_{11}$ eq] | 6.6 | 5.1 | 4.7 | 4.9 | 4.7 | 4.6 | 4.7 |
| | Fine particulate matter formation | PMFP x 10 [mg PM2.5 q] | 5.5 | 4.2 | 3.8 | 4.2 | 4 | 3.9 | 4 |
| | Ecosystem damage ozone formation | EOFP x 10 [mg NOx eq] | 7.1 | 5.3 | 4.8 | 5.4 | 5.2 | 5.1 | 5.1 |
| | Human damage ozone formation | HOFP x 10 [mg NOx eq] | 6.9 | 5.2 | 4.8 | 5.3 | 5.1 | 5 | 5.1 |

**Note:** The stronger the blue shades, the lower the impact; the stronger the red shade, the higher the impact.

**Table 7**
Environmental impacts by system: water and land pollution, toxicity and energy recovery.

| Group | Impact category | Acronyms [Unit] | PERC | PERC+ | TOPCon | HJT 1 | HJT 2 | HJT 3 | HJT 4 |
|---|---|---|---|---|---|---|---|---|---|
| **Water and land pollution** | Terrestrial acidification | TAP x 10 [kg SO2 eq.] | 15.4 | 11.8 | 10.7 | 11.8 | 11.1 | 11 | 11.1 |
| | Freshwater eutrophication | FEP [mg P eq.] | 9.7 | 7.9 | 7.5 | 7.9 | 7.6 | 7.3 | 7.4 |
| | Marine eutrophication | MEP [mg N eq.] | 3.8 | 3 | 2.6 | 2.8 | 2.7 | 2.6 | 2.6 |
| **Toxicity** | Human toxicity: Cancer | HTPc [g 1,4-DCB] | 2.6 | 2.1 | 2 | 2 | 1.9 | 1.9 | 1.9 |
| | Human toxicity: non-cancer | HTPnc x 10 [g 1,4-DCB] | 5.3 | 4.5 | 4.3 | 4.6 | 4.5 | 4.2 | 4.2 |
| | Terrestrial Ecotoxicity | TETP x 10 [g 1,4-DCB] | 14.6 | 12.2 | 11.6 | 12.4 | 12.1 | 11.7 | 11.8 |
| | Freshwater Ecotoxicity | FETP [g 1,4-DCB] | 1.1 | 1 | 0.9 | 1 | 1 | 0.9 | 0.9 |
| | Marine Ecotoxicity | METP [g 1,4-DCB] | 1.7 | 1.4 | 1.4 | 1.4 | 1.4 | 1.3 | 1.3 |
| | Ionising Radiation | IRP [Bq Co-60eq] | 3.2 | 2.4 | 2.3 | 2.2 | 2.1 | 2.1 | 2.1 |
| **Energy recovery** | Energy Payback Time | EPBT [years] | 2.3 | 1.8 | 1.6 | 1.7 | 1.6 | 1.6 | 1.6 |

**Note:** The stronger the blue shades, the lower the impact; the stronger the red shade, the higher the impact.

impacts in 11 out of 19 categories. The TOPCon technology is the second-best performer, showing lower impacts in 8 out of 19 categories.

### 4.1.1. Climate change (GWP_{100})

As seen in Table 6, among the systems evaluated, the PERC system has the highest impact with emissions estimated at 25.6 g $CO_2$ eq./kWh, while HJT 3 shows the lowest impact at 17.6 g $CO_2$ eq/kWh; HJT 3 is closely followed by TOPCon and HJT 4 (17.8 g $CO_2$ eq/kWh) and HJT 2 (17.9 g $CO_2$ eq/kWh). Between 84% and 94% of the contributions to $GWP_{100}$ are concentrated in the production of the wafer, the module, and the BOS across all systems. The wafer manufacturing stage contributes by up to 40%, which is mainly due to the energy required (and source of it) in the manufacturing of solar-grade silicon and ingots. The module manufacturing stage adds 24–27% mainly because of the glass fabrication, the module assembly, and the production and sourcing of aluminium frames. Finally, the BOS stage counts for 23–27% of CC, where emissions from the manufacturing of assembly structures (aluminium and steel) and inverters are the main contributors.

The differences in $GWP_{100}$ between PERC, TOPCon, HJT 4 and HJT 3 technologies are notable (25.6 vs 19.4, 17.8, and 17.6 g $CO_2$ eq./kWh respectively), which is due to system design differences. For example, PERC and TOPCon modules include aluminium frames, contributing significantly to $GWP_{100}$. HJT 3, lacking a frame, reduces its environmental impact by minimising aluminium use – a material with a considerable $GWP_{100}$ – in between 1.3 and 1.8 g $CO_2$ eq/kWh. This design choice specifically addresses a major hotspot in PV manufacturing. As shown in Table 1, standard modules (PERC, TOPCon) incorporate aluminium frames weighing approximately 2.13 kg per module. By eliminating this component, the HJT 3 design avoids the high energy intensity associated with primary aluminium production and its subsequent extrusion, which are significant contributors to the carbon footprint in the other studied systems. However, HJT 3 incorporates thicker glass, leading to a 92% increase in its $GWP_{100}$

contribution compared to TOPCon, because of high resource and energy consumption in glass manufacturing processes. The production of aluminium and steel for mounting structures significantly affects $GWP_{100}$, accounting for approximately 10% and 5% of $GWP_{100}$ respectively across all systems. Although aluminium has a greater impact, both materials are considerable contributors to the overall sustainability of PV systems. Finally, the manufacturing of all components predominantly occurs in China, where the electricity mix has a high proportion of coal-based generation (64.7% in 2019), further influencing the environmental impacts (Our World in Data, 2025).

Regarding the intermediate performance of the PERC+ technology, its significant advantage over the standard PERC system (19.4 vs 25.6 g $CO_2$ eq/kWh) is primarily driven by its advanced cell architecture. As detailed in Table 1, PERC+ incorporates a bifacial factor of 70% and half-cut cell technology, which together boost the module efficiency to 20.24%, compared to 17.46% for the monofacial PERC. This increased energy yield significantly dilutes the environmental burden per functional unit. However, PERC+ still presents a higher impact than the HJT variants (specifically HJT 3 at 17.6 g $CO_2$ eq/kWh) due to material intensity. Unlike the frameless HJT 3 design, the PERC+ module retains an aluminium frame (2.13 kg/m), contributing to a higher embodied carbon footprint in the manufacturing stage.

### 4.1.2. Resource scarcity

As displayed in Table 6, PERC, HJT 1 and HJT 2 systems have the greatest SOP, with 171, 169 and 163 mg Cu eq./kWh, respectively. In contrast, HJT 3&4, which use smart-wire metallisation technology, show the lowest impact (127 and 128 mg Cu eq./kWh), highlighting their efficiency in mineral resource use. Approximately 97% of the impacts are concentrated in the BOS, and cell and module manufacturing stages. BOS accounts for between 43 and 56% due to a significant use of copper in the inverters (15–18%) and electrical conductors (15–17%), together with the steel used in mounting structures (11%). In the case of

the cells manufacturing stages, their contribution represents 24–41%. For HJT 1 and HJT 2, silver contacts increase SOP, due to the use of standard busbar metallisation (4BB and 6BB, respectively), whereas for HJT 3 and HJT 4 the use of Smart-Wire Connection Technology (SWCT) reduces the amount of silver required, making these technologies more competitive in relation to SOP. Unlike traditional busbars that require silver paste printing for electrical contacts, the SWCT uses a matrix of copper wires coated with a low-temperature alloy. This architecture allows for a drastic reduction in silver consumption – a critical raw material with high depletion potential – thereby driving the superior performance of HJT 3 (127 mg Cu eq./kWh) compared to HJT 1 (169 mg Cu eq./kWh). Finally, the module manufacturing stage's contribution (13–20%) refers to the copper and tin used in cell interconnection.

A similar trend is seen in WCP, where the PERC system displays the highest impact (83 L/kWh), while HJT 2–4 show the lowest impact (~58 L/kWh). The variation between the other technologies is very narrow in comparison to the best performers – less than 7 L/kWh.

FFP and LOP show a comparable tendency. The higher impacts are seen in the PERC system (5.7 g oil eq./kWh and 118 $cm^2$ y eq./kWh), while the lowest are seen in the TOPCon system (4 g oil eq./kWh and 87 $cm^2$ y eq./kWh). Similarly, regarding Mineral Resource Scarcity (SOP), PERC+ (14.2 mg Cu eq.) improves upon PERC (17.1 mg Cu eq.) due to efficiency gains, but remains inferior to HJT 3 (12.7 mg Cu eq.). This gap is attributed to the metallisation technology: PERC+ utilises a standard multi-busbar (9BB) interconnect which is more silver-intensive than the SWCT (18BB) employed in HJT 3. The rest of the systems present similar orders of magnitude for both FFP (4.1–4.3 g oil eq./kWh) and LOP (93–95 $cm^2$ y eq./kWh), except for HJT 1 that presents a higher LOP (100 $cm^2$ y eq./kWh).

### 4.1.3. Air pollution

TOPCon and HJTs technologies, especially HJT 3, have the lowest impacts across all air pollution impact categories (see Table 6). PERC system is by far the worst performer, with impacts 40–48% higher than

the best performer (TOPCon and HJT 3). PERC system exhibits the highest ODP with 6.6 µg $CFC_{11}$ eq./kWh while HJT 3 shows the lowest with 4.6 µg $CFC_{11}$ eq./kWh. TOPCon and HJT 2 and 4 present similar ODP than HJT 3, only 2.3% higher. The main contributor to this impact is the emissions of $N_2O$, which for HJT 3 represent ~85%. PMFP ranges from 39 (TOPCon) to 55 (PERC) mg PM2.5 eq./kWh, and it is significantly influenced by the production of solar-grade silicon and ingots, due to the energy requirements of high-temperature processes and to the chemical materials usage. Glass manufacturing for the modules is another considerable PMFP source, surpassing emissions from the aluminium frame production, mainly due to the high temperature melting of sand. In contrast, the aluminium manufacturing process generates higher emissions of greenhouse gases ($CO_2$) and perfluorocarbons (PFCs), derived from alumina electrolysis used for the mounting structures as part of the BOS.

### 4.1.4. Water and land pollution

As seen in Table 7, the PERC system displays the highest environmental impact across all water and land impact categories, between ~33% (for FEP) and 46% higher (for MEP) than the best performer. TOPCon and HJT 3 exhibit the lowest impacts, positioning them as the best performers in this impact group. The rest of the systems, PERC+ and HJT 1,2 and 4, show impacts in the lower end, with values only up to 15% higher than TOPCon and HJT 3.

In the case of the PERC system, the largest contributor to TAP, estimated at 154 kg $SO_2$ eq./kWh, is $SO_2$ emissions from the energy consumption of the solar silicon and ingots production, key activities of the wafer manufacturing stage. In the case of HJT 3 (107 kg $SO_2$ eq./kWh), the major contributors to TAP are also the wafer production (43%), followed by the module production (26%), and BOS and installation (21%) stages, due to emissions associated with the extraction of aluminium and copper.

The PERC system also shows the highest FEP, calculated at 9.7 mg P eq./kWh, indicating greater contributions to nutrient accumulation in
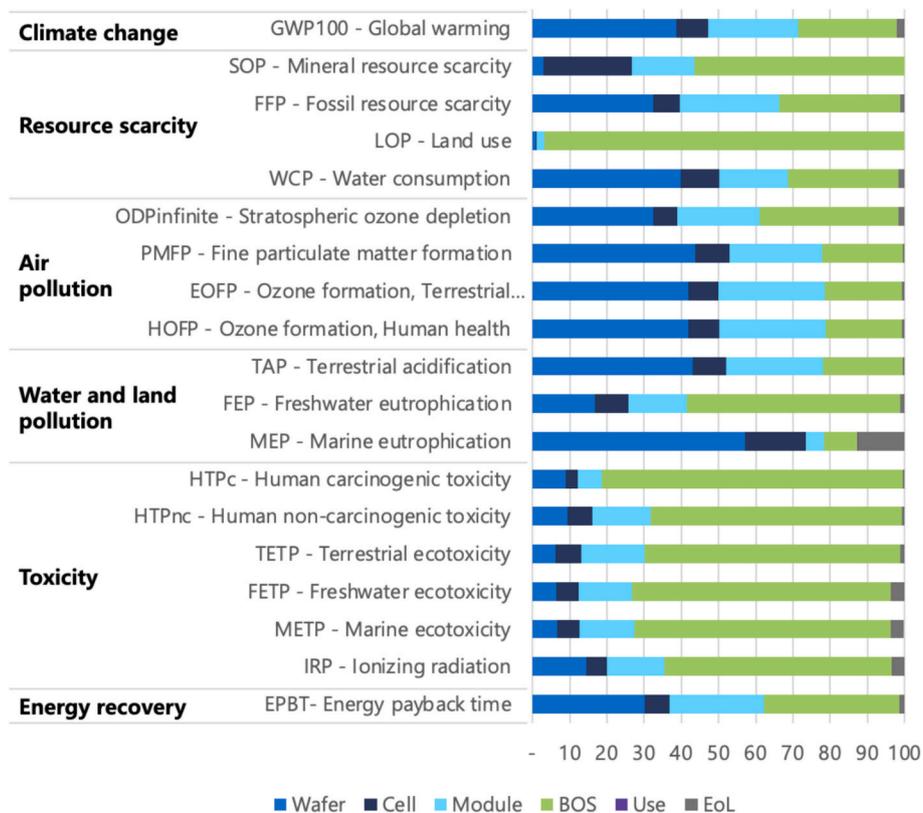


**Fig. 2.** Contribution of each life cycle stage to the environmental Impact of HJT 3. See SI for impact contribution of PERC, PERC+, TOPCon and HJT 1–4.

**Table 8**
Key component composition and recycling rate accounted for in HTJ 3 system.

| Component | Material | Component | Weight [t] | Recycling rate |
|---|---|---|---|---|
| Module | Glass | 91% | 48.1 | 90% |
| | Plastics | 5% | 2.6 | 0% |
| | Cell | 3% | 1.6 | 0% |
| | Copper | 1% | 0.3 | 80% |
| | Others | 1% | 0.5 | 0% |
| | **Subtotal** | **100%** | **53.1** | **82%** |
| Mounting structure | Steel | 57% | 21.6 | 70% |
| | Aluminium | 32% | 12 | 80% |
| | Concrete | 10% | 3.9 | 0% |
| | Others | 2% | 0.6 | 0% |
| | **Subtotal** | **100%** | **38.2** | **65%** |
| Inverter | Steel | 50% | 3.4 | 70% |
| | Oil | 31% | 2.1 | 70% |
| | Copper | 12% | 0.8 | 80% |
| | Aluminium | 5% | 0.3 | 80% |
| | Others | 4% | 0.2 | 0% |
| | **Subtotal** | **100%** | **6.8** | **69%** |
| Electrical installation | Copper | 47% | 0.7 | 80% |
| | Plastics | 49% | 0.8 | 0% |
| | Steel | 3% | 0.1 | 70% |
| | Others | 0% | 0 | 0% |
| | **Subtotal** | **100%** | **1.6** | **40%** |
| | **TOTAL** | | **99.7** | **74%** |

water bodies due to phosphate emissions from metal and coal mining waste disposal, driven by the extraction and processing of raw materials used in the manufacturing of inverters, mounting structures, and electrical conductors of the BOS stages. HJT 3 and HJT 4 exhibit the lowest FEP, partly due to higher efficiency and other factors. For instance, for HJT 3, wastewater treatment during copper production accounts for 38% of FEP, BOS structures contribute 19%, and the copper in the module interconnections adds 7%.

For MEP, all systems except PERC show similar impacts (2.6–3 mg N eq∕kWh). The greatest burden comes from waste management, particularly wastewater treatment in the ingot production (54%), followed by the cell manufacture (16%) and end-of-life management (12%).

### 4.1.5. Toxicity impacts

As shown in Table 7, HJT 3 exhibits the lowest impact across all toxicity related categories. In HJT 3, ~70% of the toxicity related impacts are concentrated in the BOS and installation stage, due to emissions of copper (66%), zinc (15%), nickel (7%), and silver (4%) generated during the production of metal components, primarily from the manufacturing of inverters, mounting structures, and electrical conductors.

The major contributions to HTPc and IRP are from steel and aluminium production for the assembly structures, accounting for 51–66% of these impacts across all systems. Copper and zinc emissions from copper production for inverters and electrical installations are important contributors to HTPnc, TETP, FETP, and METP, representing 50–57% of the impacts.

### 4.1.6. Energy recovery

As seen in Table 7, HJT 2,3 and 4 have the shortest EPBT estimated at ~1.6 years, making these systems the most efficient in returning the energy used in their life cycle. Conversely, the PERC system has the longest EPBT, calculated at 2.31 years. In HJT 3, the BOS and installation stages are the most energy-demanding phases (36% of EPBT), followed by the wafer (30%) and module (25%) stages. Cell manufacturing contributes 7%, while the end-of-life stage has the lowest contribution.

### 4.1.7. Hotspot analysis

After quantifying the environmental impacts, we performed a hotspot analysis, evaluating the contribution of each life cycle stage to the environmental load of the seven PV systems studied. Given that HJT 3 is
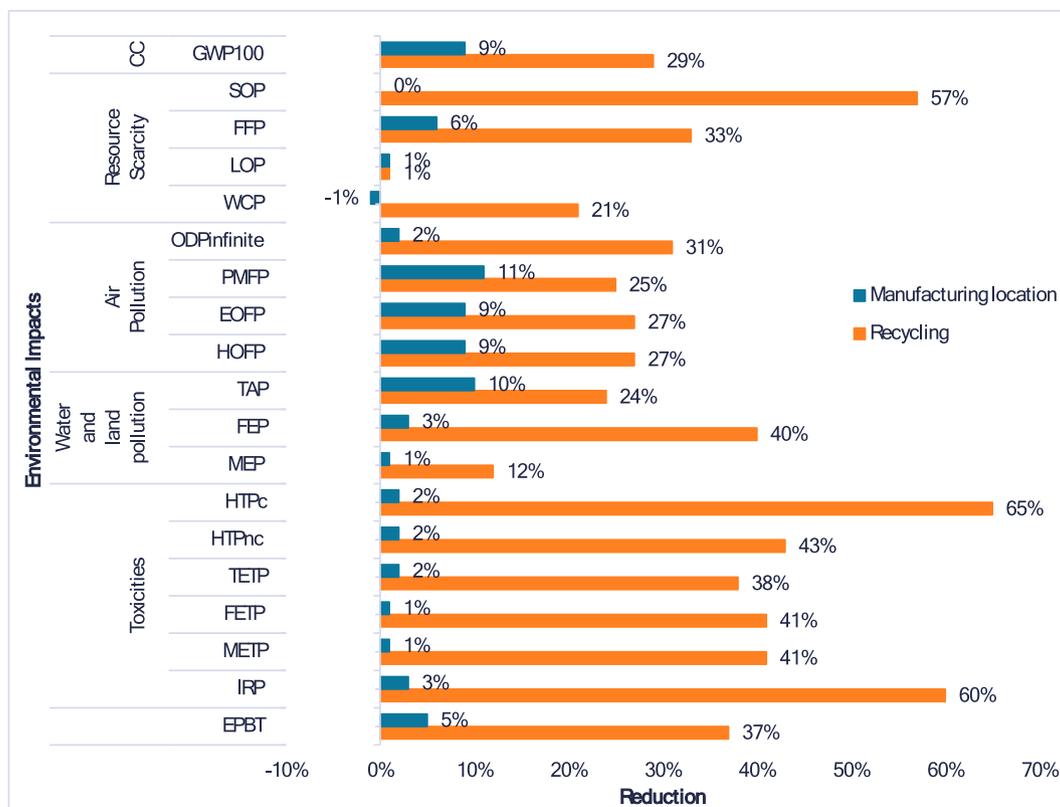


**Fig. 3.** Scenario analysis - changes in the environmental impacts by modifying end-of-life stage (orange) and manufacturing location (blue) for the HJT 3 design (see SI for absolute values).

the most environmentally sustainable option, we use it as a reference to assess the contributions of different life cycle stages across various impact categories. The results are presented in Fig. 2. The contribution of all other technologies can be found in the Supplementary Information, Table S1–18. The Balance of System (BOS) and installation stage shows the greatest impact on PV systems, contributing 46% on average across all environmental burden. This stage presents significant impacts in 12 environmental categories, including toxicities (~69%), LOP (~97%), FEP (~57%), SOC (~56%), ODP (~37%), and EPBT (~36%). The wafer manufacturing stage follows in level of importance, representing ~25% of the total environmental load. This stage greatly contributes to $GWP_{100}$ (~39%), WCP (~40%), air pollution categories (~40%), MEP (~57%), and FFP (~33%). The module manufacturing stage contributes ~18%, with important contributions in $GWP_{100}$ (~24%), air pollution (~26%) and FFP (~27%). The cell manufacturing stage displays an average share of 8%, standing out for SOP, representing 24% of its impact. The use and end-of-life stages present negligible contribution across almost all impact categories, except for MEP, where the end-of-life stage represents 12% of the impacts.

### 4.2. Scenario analysis

Two scenarios have been developed to explore key aspects of the systems - the recycling content of the materials at the end of their life and the possibility of manufacturing the panels in Chile. These scenarios are described and discussed in section 4.2.1 and 4.2.2, respectively.

#### 4.2.1. End-of-life recycling

Landfilling is the current practice for the end of life of PV systems in Chile, the baseline of this study. However, commitments towards more circular economy inspired practices are starting to affect the way products are designed and their waste management, as a new regulation is enacted (Extended Product Responsibility, or Ley REP for its Spanish acronym (Ministerio del Medio Ambiente, 2025)). Therefore, it is important to study how new end-of-life practices will change the environmental impacts of PV systems. Hence, this scenario accounts for the

recycling of key materials such as glass (90%), aluminium (80%), copper (80%) and steel (70%), following practices in (Sinha et al., 2023; Heath et al., 2016). Details of the recycling rates and materials can be seen in Table 8.

As seen in Fig. 3, recycling key components of the HJT PV systems results in an average environmental burden reduction of 34%. The most substantial reductions are observed in toxicity and resource scarcity indicators. Specifically, SOP decreases by ~57%, indicating a significant drop in the depletion of mineral resources by reducing the use of virgin materials. Other notable improvements include a 24% cutback in TAP and 44% in FEP. Regarding $GWP_{100}$, recycling leads to a reduction of 5.3 g $CO_2$ eq/kWh (~29%). Air pollution indicators such as PMFP and ODP∞ decrease by 25% and 31%, respectively. Human toxicity potential shows the greatest improvements, with HTPc reduced by 65% and HTPnc by 43%. Finally, ecotoxicity categories decrease by up to ~40% each.

#### 4.2.2. Local production versus production in China of HJT modules

The environmental impact of assembling HJT PV modules in Chile, using the local electricity mix, has been evaluated against production in China, with results shown in Fig. 3. In 2019, China relied on coal for approximately 65% of its electricity generation, while Chile reduced its coal dependency from 37% to 23% over three years and increased its PV generation to 20% by 2023.

The results indicate that assembling HJT modules in Chile reduces the environmental burden by an average of 4%, particularly $GWP_{100}$ (9%), resource scarcity and air pollution impacts. FFP decreases by 6%, although there is no significant change in SOP. WCP increases by 1% due to Chile's higher proportion of hydroelectric power, which, despite being renewable, involves substantial water usage.

Local manufacturing positively influences air quality, evidenced by an 11% reduction in PMFP and a 9% reduction in EOFP and HOFP. FEP and MEP decrease by 3% and 1%, respectively, indicating reduced nutrient runoff and protection of aquatic ecosystems. Modest reductions of 1–2% are observed in HTPc and HTPnc, as well as in TETP, FETP, and METP, implying benefits for human health and biodiversity. A 3%
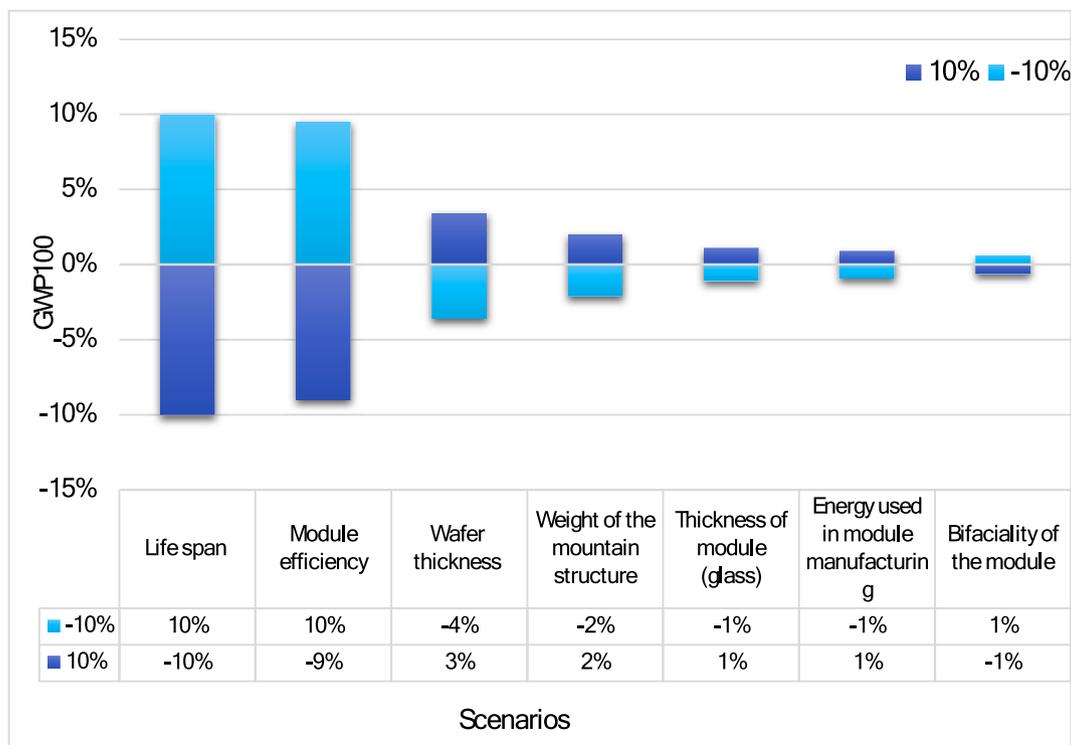


| | Life span | Module efficiency | Wafer thickness | Weight of the mountain structure | Thickness of module (glass) | Energy used in module manufacturing | Bifaciality of the module |
|---|---|---|---|---|---|---|---|
| -10% | 10% | 10% | -4% | -2% | -1% | -1% | 1% |
| 10% | -10% | -9% | 3% | 2% | 1% | 1% | -1% |

**Fig. 4.** Sensitivity analysis – results for $GWP_{100}$ for the HJT-3 design.

**Table 9**

Comparison of the environmental impacts of HJT 3 (this study), 1 MW PV system in Chile, and the national grid (Soler et al., 2025), presented per 1 kWh. Blue and yellow shadings represent lower and higher impacts, respectively.

| Impact category | HJT 3[b] | 1 MW case [19] | Variation[c] | National grid [19] |
|---|---|---|---|---|
| Global warming (GWP100) [kg $CO_2$ eq] | 1.76E-02 | 3.31E-02 | -46.83% | 3.61E-01 |
| Mineral resource scarcity (SOP) [kg Cu eq] | 1.27E-04 | 8.33E-04 | -84.76% | 5.00E-04 |
| Fossil resource scarcity (FFP) [kg oil eq] | 4.05E-03 | 8.97E-03 | -54.84% | 1.06E-01 |
| Water consumption (WCP) [m³] | 5.72E-02 | 4.49E-04 | 12639.2% | 3.59E-03 |
| Stratospheric ozone depletion (ODPinf) [kg CFC11 eq] | 4.64E-09 | 1.30E-08 | -64.31% | 1.65E-07 |
| Fine particulate matter formation (PMPF) [kg PM2.5 eq] | 3.93E-05 | 8.26E-05 | -52.42% | 2.34E-03 |
| Ozone formation – Human health (HOFP) [kg $NO_x$ eq] | 5.01E-05 | 1.09E-04 | -54.03% | 1.20E-03 |
| Ozone formation – Terrestrial ecosystems (EOFP) [kg $NO_x$ eq] | 5.09E-05 | 1.12E-04 | -54.55% | 1.30E-03 |
| Terrestrial acidification (TAP) [kg $SO_2$ eq] | 1.10E-04 | 1.98E-04 | -44.44% | 1.91E-03 |
| Freshwater eutrophication (FEP) [kg P eq] | 7.33E-06 | 2.60E-05 | -71.77% | 1.39E-04 |
| Marine eutrophication (MEP) [kg N eq] | 2.06E-06 | 1.62E-06 | 27.16% | 7.75E-06 |
| Human carcinogenic toxicity (HTPc) [kg 1,4-DCB eq] | 1.86E-03 | 6.52E-03 | -71.48% | 1.37E-02 |
| Human non-carcinogenic toxicity (HTPnc) [kg 1,4-DCB eq] | 4.20E-02 | 1.73E-01 | -75.73% | 2.50E-01 |
| Terrestrial ecotoxicity (TETP) [kg 1,4-DCB eq] | 1.17E-01 | 7.33E-01 | -84.06% | 1.07E+00 |
| Freshwater ecotoxicity (FETP) [kg 1,4-DCB eq] | 9.00E-04 | 1.17E-02 | -92.31% | 1.45E-02 |
| Marine ecotoxicity (METP) [kg 1,4-DCB eq] | 1.32E-03 | 1.52E-02 | -91.32% | 1.90E-02 |
| Ionising radiation (IRP) [kBq Co-60 eq] | 2.05E-03 | 1.33E-03 | 54.14% | 2.08E-03 |

[a] Only 17 impacts are compared as LOP and EPBT were not included in (Soler et al., 2025); [b] HJT 3 - best performer of this study. For description, see Table 1; [c] Comparison between HJT 3 and PV System (Soler et al., 2025).

reduction in IRP is also noted. Interestingly, the EPBT increases by 5%, suggesting improved energy efficiency in the production process.

### 4.3. Sensitivity analysis

A sensitivity analysis was conducted to evaluate how changes (±10%) in key parameters of PV modules affect their environmental impact. The parameters examined include the lifetime, module efficiency, wafer thickness, weight of mounting structures, glass thickness of the modules (both front and back), energy used in module manufacture, and module bifaciality. A selection of environmental indicators commonly used to inform design, and manufacturing choices (Kourkoumpas et al., 2018) are included in the analysis to enable a thorough discussion and to provide better understanding of the effect on them. These indicators are $GWP_{100}$, Mineral Resource Scarcity (SOP) and Energy Payback Time (EPBT).

As shown in Fig. 4, results indicate that $GWP_{100}$ is highly sensitive to changes in PR, irradiance, lifetime, and module efficiency, with variations in $GWP_{100}$ of up to ±10%. This trend is consistent across SOP and EPBT, as all three metrics are primarily driven by the system's total energy generation (the denominator of the functional unit). For GWP100, these variations range from 2% to 3.4%. Similarly, for SOP, while the mounting structure represents a relevant share of the mineral depletion, the sensitivity to a ± 10% change in its weight remains limited (~1%), confirming that efficiency gains are the most effective lever for reducing environmental burdens across all categories.

Changes in glass thickness, energy used in module manufacture, and module bifaciality show lower variability (< 1.5%) across all indicators. This suggests that while design optimisation is important, the environmental performance is fundamentally determined by the site conditions (irradiance) and the core efficiency of the PV technology.

### 4.4. Validation of results

The validation of the results is carried out using studies from the Chilean context, namely Soler et al. (Soler et al., 2025) who carried out a LCA study of 1 MW utility-scale photovoltaic installation and of the 2024 Chilean national electricity mix. This study has been chosen because the geographical proximity of these systems, all located in the Antofagasta region, ensures consistency in solar resource assumptions and the environmental background conditions. Table 9 summarises the midpoint impact indicators according to the ReCiPe 2016 (H) method using 1 kWh as reference unit.

As seen in Table 9, the HJT3 system exhibits lower environmental impacts than those estimated for the 1 MW case by Soler et al. (Soler et al., 2025) in most categories, 13 out of 18, driven primarily by its higher energy conversion efficiency (26.6% vs. 17%) and updated production technologies. Nonetheless, several categories show substantial deviations from this trend i.e., WCP, MEP, IRP, which can be explained by differences in inventory completeness, geographic assumptions, and energy sourcing. In relation to the national grid, which has been added here for reference, the HJT3 shows lower environmental impacts across

all the impact categories.

For climate change, GWP, the comparison shows that this study is 46% lower than that of Soler et al. (Soler et al., 2025), which is consistent with the higher electricity output per material and energy input in the HJT3 system, validating the expected performance gains from greater efficiency. This also explains the better performance of HJT3 in impacts such as FFP (~54%) and ozone formation indicators (~54%).

Important reductions are also seen in mineral resource scarcity (~85%) due to decreased demand for silver, copper, and aluminium per kWh, enabled by more efficient metallisation and design optimisation of the HJT3 modules. Similarly, ecotoxicity indicators show important reductions (up to ~92%), as the more recent inventory used in this study includes updated background processes with reduced emissions of heavy metals and solvents, particularly in wafer production and encapsulation steps. Human toxicity impacts also see a better performance in this study, with reductions of up to ~76% when comparing with Soler et al. (Soler et al., 2025). These reductions stem from cleaner chemical inputs and tighter control of emissions in Chinese manufacturing chains, as reflected in the updated Ecoinvent data. EP decreases in HJT3 when comparing with the previous study (~72%). Improved wastewater management and lower phosphorus discharges in polysilicon purification stages contribute to this result.

Three categories worsen for HJT3. WCP increases by ~127 times. This significant discrepancy is primarily driven by the comprehensive accounting of the indirect water footprint associated with the Chinese electricity mix used for upstream manufacturing. Unlike the comparative study (Soler et al., 2025), which limits its scope to direct industrial water consumption, our inventory utilises Ecoinvent datasets that quantify the water usage associated with hydroelectric power generation (reservoir evaporation and turbined water). Importantly, the ReCiPe 2016 impact assessment method explicitly accounts for these flows, resulting in a significantly higher WCP value that accurately reflects the water intensity of the grid-dependent supply chain. Although in smaller order of magnitude, IR increases by ~54% when compared with the literature. This is because the electricity mix used in the Chinese upstream manufacturing processes includes a higher share of nuclear energy compared to the European mix assumed in Soler et al. (Soler et al., 2025). Finally, ME increases by 27% due to greater nitrogen emissions associated with upstream production stages, particularly those involving ammonia and nitrate-bearing compounds in cleaning and etching processes.

### 4.5. Limitations

The limitations of this study rely mainly on the assumptions made to build inventories and to represent real-life systems as accurate as possible when modelling, and on the temporal aspects of the databases used.

We have used Ecoinvent models from v 3.9.1 as basis of the systems. This was the best approach available at the time of the study. Adaptations to these models were made to represent our systems using manufacturers' manuals, modelling software, literature, and on-site experiments. However, receiving data directly from the manufacturers of each component and from on-site installations would have been ideal to reduce assumptions and therefore uncertainties.

At the time of this study, we only had access to Ecoinvent v3.9.1. We are aware that when publishing this study, the latest version available will have been v12. This is an important limitation, as updates or new available models could incorporate improvements, or provide more closely related models that could affect the results of this study.

Finally, we have identified that BOS is an important contributor to the environmental impacts of the system. For modelling purposes, Ecoinvent modules were used as background for the inventories, modified accordingly to specifications of the system. However, using detailed information from manufacturers and/or installations would provide a better understanding of each component, in order to reduce uncertainty of the results, and to provide specific design and installation recommendations.

### 5. Conclusion

This study provides a detailed environmental impact assessment of four PV systems using novel PV module designs for extreme environments such as the Atacama Desert. The results show that HJT 3 systems achieve up to 30% lower $GWP_{100}$ per kWh of electricity generated, compared to conventional monofacial PERC modules. This reduction is driven by three synergistic design features specific to the HJT 3 module: 1) Its frameless configuration, which eliminates the carbon-intensive aluminium burden found in conventional modules, 2) the use of Smart-Wire Connection Technology (SWCT), which minimises the consumption of critical minerals, specifically silver, compared to standard busbar designs, and 3) a superior bifaciality (91%) combined with high conversion efficiency (19.1%), which maximises energy yield and dilutes the environmental impact per functional unit.

A key finding is that the Balance of System (BOS) components account for approximately 46% of the total environmental burden, with mounting structures and inverters being major contributors. Future reductions in environmental impact could be achieved by optimising BOS materials, integrating more efficient inverters, and incorporating sustainable manufacturing practices. Additionally, circular economy practices and increasing recycling rate of materials will be key to reduce impacts of PV systems.

Compared to TOPCon technology, ATAMO - HJT modules also demonstrate notable advantages. HJT 3 modules show approximately 15% lower $GWP_{100}$ than TOPCon modules, primarily due to higher efficiency and reduced material consumption. Additionally, TOPCon's reliance on silver for metallisation contributes to higher SOP, while HJT 3 modules, with their smart-wire metallisation, mitigate this issue. However, TOPCon modules exhibit marginally lower environmental impacts in certain categories, such as ODP, due to differences in production energy sources.

Recycling presents a significant opportunity for impact reduction. The results of the scenario analysis indicate that recovering and reusing key materials such as aluminium, steel, copper, and glass can reduce environmental burdens by an average of 34%. Specifically, under high-recycling scenarios, mineral resource depletion decreases by 57%, terrestrial acidification by 24%, and freshwater eutrophication by 44%. Additionally, local assembly of PV modules in Chile could reduce the $GWP_{100}$ by up to 9% by leveraging the country's cleaner energy mix.

These results highlight the importance of measuring the potential environmental impacts considering all relevant stages of the life cycle, which is currently not the case when assessing technologies in Chile. Specifically, as solar energy adoption accelerates, addressing its environmental footprint is imperative. The quantitative results of this study suggest that improving PV sustainability in Chile requires policy attention to performance per kWh, non-module components, and credible end-of-life pathways, not only module choice. Based on our results, we present the following policy recommendations for both upstream and downstream (end of life) stages:

- Shift procurement and evaluation towards delivered electricity (kWh) and durability in desert conditions: Because HJT 3 achieves up to 30% lower GWP100 per kWh through higher efficiency and design choices, and because results are highly sensitive to PR, irradiance, lifetime, and efficiency, public tenders and large-scale project approvals should require transparent reporting of these parameters.
- Make Balance of System (BOS) a core sustainability target: Since BOS and installation contribute ~46% of the total environmental burden on average, policy instruments, such as procurement rules and technical standards, must explicitly cover mounting structures and

inverters – e.g. requiring material-efficiency specifications and minimum documentation for major BOS items.

- Incentivise Eco-Design through Eco-Modulation: Regulations should operationalise 'eco-modulation' mechanisms that lower compliance fees for producers who adopt designs with high recyclability and low critical mineral intensity. As demonstrated in this study, technologies like the frameless, low-silver HJT 3, significantly reduce the environmental burden of material recovery (e.g. HJT 3 presents a 25% reduction approximately in Mineral Resource Scarcity compared to PERC) and should be fiscally favoured over material-intensive designs. Durability, critical material intensity, and verified recovery performance are practical candidate parameters to assess this.

- Integrating eco-design principles in existing and new PV panels and PV systems design, development and manufacturing, aligning with Chile's recently updated law on Extended Producer Responsibility (EPD) (in Spanish *Ley de Responsabilidad Extendida del Productor (REP): Ley Marco 20.920 para la gestión de residuos*) (Ministerio del Medio Ambiente, 2025). This new amendment adds PV panels into the list of product categories under the law and sets requirements to manufacturers about end-of-life management of PV panels. The law requires an end-of-life recycling capacity of 10% for the first 3 years, to get to 50% of recycling in 10 years. As shown in this study, recovering and reusing key materials such as aluminium, steel, copper, and glass can reduce environmental burdens by an average of 34%. In high recycling scenarios, mineral resource depletion, terrestrial acidification, and freshwater eutrophication could decrease by 57%, 24%, and 44%, respectively. Policies should enforce measurable outcomes, with minimum collection rates and verified recovery rates by material, using this study's scenario values (e.g., high recovery of glass and major metals) as indicative initial benchmarks.

- Leverage the Extended Producer Responsibility (EPR) Law with verified circular pathways: With the enactment of the Decree for Batteries and Electrical and Electronic Equipment (approved by the Council of Ministers in June 2025) – which explicitly classifies photovoltaic modules as a priority subcategory of Waste from Electrical and Electronic Equipment (WEEE) with specific collection targets scaling to 50% by the tenth year – priority must be given to establishing certified recycling infrastructure in the northern regions. Policy must ensure (i) clear responsibility for take-back, (ii) certified treatment routes, and (iii) reporting that demonstrates real recovery rather than "paper compliance".

Aligning procurement, permitting, and REP-style obligations around these priorities would help ensure that rapid solar expansion in Chile's desert context translates into durable and verifiable broad sustainability gains.

## CRediT authorship contribution statement

**Jose Maria Cruz:** Writing – original draft, Validation, Software, Methodology, Investigation, Formal analysis, Conceptualization. **Ximena Schmidt Rivera:** Writing – original draft, Validation, Supervision, Methodology, Conceptualization. **Francisca Jalil-Vega:** Writing – review & editing, Writing – original draft, Supervision. **Raúl O'Ryan:** Writing – original draft. **Felipe Valencia:** Project administration. **Jorge Rabanal-Arabach:** Project administration. **Eduardo Ayllón Opazo:** Investigation. **Paulina Andrea Morris Carmona:** Investigation. **Patricio Larrain Yañez:** Investigation.

## Declaration of competing interest

The authors declare that they have no known competing financial interests or personal relationships that could have appeared to influence the work reported in this paper.

## Appendix A. Supplementary data

Supplementary data to this article can be found online at https://doi.org/10.1016/j.spc.2026.03.004.

## References

ACERA A.G, 2023. Centro de información: mapa de proyectos ERNC en Chile [cited 2023 31 October]; Available from: https://www.acera.cl/mapa-de-proyectos/.

Adiansyah, J.S., Agusdinata, D.B., Putra, A.P., 2025. Environmental impacts of solar PV energy systems for small-island communities in Indonesia: a life cycle assessment approach. Energy Sustain. Dev. 85, 101651.

Akram Cheema, H., Ilyas, S., Kang, H., Kim, H., 2024. Comprehensive review of the global trends and future perspectives for recycling of decommissioned photovoltaic panels. Waste Manag. 174, 187–202.

Alexis, B., 2022. Life Cycle Assessment of Heterojunction Solar Cells. From Raw Materials to Final Devices.

Atamostec, 2023. Desarrollo de tecnologías para la industria solar fotovoltaica en climas desérticos y de alta radiación [cited 2025 02 February]; Available from: https://www.atamostec.cl/sitio/.

Coordinador Eléctrico Nacional, 2023. Informes de Mínimos Técnicos Unidades Generadoras [cited 2023 31 October]; Available from: https://www.coordinador.cl/parametros-operacionales/documentos/minimo-tecnico/informes-de-minimos-tecnicos-unidades-generadoras/.

Cordero, R.R., Feron, S., Sepúlveda, E., Damiani, A., Carrera, J.M., Jorquera, J., Alfonso, J.A., Fuenzalida, R., Rivas, M., MacDonell, S., Seckmeyer, G., Wang, C., Ouyang, Z., Lhermitte, S., 2021. Evaluation of MODIS-derived estimates of the albedo over the Atacama Desert using ground-based spectral measurements. Sci. Rep. 11 (1), 19822.

Ecoinvent, 2023. Ecoinvent v3.9.1.

Elias Urrejola, J.T., Zambrano, Maria Jose Riquelme, Muñoz, Delfina, Kopecek, Radovan, Fuentealba-Vidal, Edward, 2020. ATAMOSTEC desert label for PV technologies. In: EU PVSEC 2020, pp. 1033–1037.

Faes, A., Despeisse, M., Levrat, J., Champliaud, J., Badel, N., Kiaee, M., Söderström, T., Yao, Y., Grischke, R., Gragert, M., Ufheil, J., Papet, P., Strahm, B., Cattaneo, G., Cattin, J., Baumgartner, Y., Hessler-Wyser, A., Ballif, C., 2014. SmartWire solar cell interconnection technology. In: 29th European Photovoltaic Solar Energy Conference. Amsterdam, The Netherlands.

Frischknecht, R., S., P., Krebs, L., de Wild-Scholten, M., Sinha, P., 2020. Life Cycle Inventories and Life Cycle Assessments of Photovoltaic Systems 2020 - Task 12 PV Sustainability. International Energy Agency.

Gaete-Morales, C., Gallego-Schmid, A., Stamford, L., Azapagic, A., 2018. Assessing the environmental sustainability of electricity generation in Chile. Sci. Total Environ. 636, 1155–1170.

Gilman, P., 2015. SAM Photovoltaic Model Technical Reference. United States.

Heath, G., Weckend, S., Wade, A., 2016. End of Life Management: Solar Photovoltaic Panels. Available from the International Energy Agency Photovoltaic Power Systems Programme (IEA-PVPS). http://www.iea-pvps.org/index.php?id=381.

Huijbregts, M.A.J., Steinmann, Z.J.N., Elshout, P.M.F., Stam, G., Verones, F., Vieira, M., Zijp, M., Hollander, A., van Zelm, R., 2017. ReCiPe2016: a harmonised life cycle impact assessment method at midpoint and endpoint level. Int. J. Life Cycle Assess. 22 (2), 138–147.

International Energy Agency, 2022. Special Report on Solar PV Global Supply Chains. OECD.

International Energy Agency, 2024. Photovoltaic Power Systems Programme, Research Task 12 - PV Sustainability. Available from: https://iea-pvps.org/research-tasks/pv-sustainability/.

International Organization for Standardization (ISO), 2006. Environmental Management — Life Cycle Assessment — Requirements and Guidelines (ISO 14044:2006).

Ito, M., Kato, K., Komoto, K., Kichimi, T., Kurokawa, K., 2008. A comparative study on cost and life-cycle analysis for 100 MW very large-scale PV (VLS-PV) systems in deserts using m-Si, a-Si, CdTe, and CIS modules. Prog. Photovolt. Res. Appl. 16 (1), 17–30.

KBOB, 2024. Life cycle assessment data in the construction sector. Available from: https://www.kbob.admin.ch/de/oekobilanzdaten-im-baubereich.

Kourkoumpas, D.-S., Benekos, G., Nikolopoulos, N., Karellas, S., Grammelis, P., Kakaras, E., 2018. A review of key environmental and energy performance indicators for the case of renewable energy systems when integrated with storage solutions. Appl. Energy 231, 380–398.

Lelièvre, J.F., Couderc, R., Pinochet, N., Sicot, L., Munoz, D., Kopecek, R., Ferrada, P., Marzo, A., Olivares, D., Valencia, F., Urrejola, E., 2022. Desert label development for improved reliability and durability of photovoltaic modules in harsh desert conditions. Sol. Energy Mater. Sol. Cells 236, 111508.

Long, J., Lu, Z., Miller, P.A., Pongratz, J., Guan, D., Smith, B., Zhu, Z., Xu, J., Zhang, Q., 2024. Large-scale photovoltaic solar farms in the Sahara affect solar power generation potential globally. Commun. Earth Environ. 5 (1), 11.

Ludin, N.A., Mustafa, N.I., Hanafiah, M.M., Ibrahim, M.A., Asri Mat Teridi, M., Sepeai, S., Zaharim, A., Sopian, K., 2018. Prospects of life cycle assessment of renewable energy from solar photovoltaic technologies: a review. Renew. Sust. Energ. Rev. 96, 11–28.

Maalouf, A., Okoroafor, T., Jehl, Z., Babu, V., Resalati, S., 2023. A comprehensive review on life cycle assessment of commercial and emerging thin-film solar cell systems. Renew. Sust. Energ. Rev. 186, 113652.

Marzo, A., Ferrada, P., Beiza, F., Besson, P., Alonso-Montesinos, J., Ballestrín, J., Román, R., Portillo, C., Escobar, R., Fuentealba, E., 2018. Standard or local solar spectrum? Implications for solar technologies studies in the Atacama desert. Renew. Energy 127, 871–882.

Ministerio del Medio Ambiente, 2025. Ley marco 20.920 para la gestión de residuos. Available from: https://economiacircular.mma.gob.cl/ley-rep/.

Molto, C., Oh, J., Mahmood, F.I., Li, M., Hacke, P., Li, F., Smith, R., Colvin, D., Matam, M., DiRubio, C., Tamizhmani, G., Seigneur, H., 2023. Review of potential-induced degradation in bifacial photovoltaic modules. Energ. Technol. 11 (4), 2200943.

Müller, A., Friedrich, L., Reichel, C., Herceg, S., Mittag, M., Neuhaus, D.H., 2021. A comparative life cycle assessment of silicon PV modules: impact of module design, manufacturing location and inventory. Sol. Energy Mater. Sol. Cells 230, 111277.

NREL, 2024. System Advisor Model (SAM). Available from: https://sam.nrel.gov/.

OpenLCA, 2025. Leading the future of LCA software [cited 2025 02 February]; Available from: https://www.openlca.org/.

Our World in Data, 2025. Share of electricity generated by fossil fuels [cited 2025 02 February]; Available from: https://ourworldindata.org/grapher/share-electricity-fossil-fuels.

Sinha, Parikhit, Raju, Sukhwant, Drozdiak, Karen, Wade, A., 2023. Life cycle management and recycling of PV systems. In: Photovoltaics International. PV TECH, pp. 26–30.

Söderströma, T., Papetb, P., Ufheilc, J., Burger, M., 2013. SmartWire Connection Technology SmartWire Connection Technology.

Soler, D., Rigamonti, L., Gazbour, N., Fuentealba, E., 2025. Environmental performance of a 1 MW photovoltaic plant in the Atacama Desert: a life cycle assessment study. Sol. Energy 292, 113454.

Song, N., Deng, S., 2022. Thin film deposition technologies and application in photovoltaics. In: Yang, D., Gibson, K. (Eds.), Thin Films - Deposition Methods and Applications. IntechOpen, Rijeka.

Ullah, F., Hasrat, K., Abdelfattah, W., Ben Khedher, N., Mu, M., Wang, S., 2025a. Comprehensive life cycle analysis of monocrystalline and polycrystalline solar PV panels in Nanjing, China: effects on the environment, performance, and recycling opportunities. Chem. Eng. J. 522, 167775.

Ullah, F., Hasrat, K., Iqbal, S., Kumar, S., Wang, S., Mu, M., Lu, W., 2025b. Evaluating the global warming potential of a 4.6 kWp solar PV system in Karak-KPK: a life cycle assessment. Appl. Therm. Eng. 266, 125790.

VDMA, 2019. International Technology Roadmap for Photovoltaic (ITRPV) 2018 Results. VDMA.

VDMA, 2020. International Technology Roadmap for Photovoltaic (ITRPV) 2019 Results. VDMA.

VDMA, 2021. International Technology Roadmap for Photovoltaic (ITRPV) 2021 Results. VDMA.

Wu, W., Chen, H., Li, C., Lu, G., Ye, D., Ma, C., Ren, L., Li, G., 2024. Assessment of the ecological and environmental effects of large-scale photovoltaic development in desert areas. Sci. Rep. 14 (1), 22456.